JOURNAL OF GEOPHYSICAL RESEARCH, VOL. 87, NO. C12, PAGES 9601–9613, NOVEMBER 20, 1982

Vertical Overturns: A Comparison of Thorpe and Ozmidov Length Scales

T. M. DILLON

School of Oceanography, Oregon State University, Corvallis, Oregon 97331

An objective measure of the length scale of turbulent overturning events, the Thorpe scale, L_T, is compared to the Ozmidov scale $L_0 = (\varepsilon/N^3)^{1/2}$, where N is the buoyancy frequency and ε is the kinetic energy dissipation rate. Far from the surface in wind-forced mixing layers and in the seasonal thermocline, L_0 and L_T are of the same order, but near the surface of a mixing layer, L_0 is significantly larger than L_T. The change in the ratio L_0/L_T is attributed to a decrease in the gradient Richardson number in the highly energetic zone near the surface. Another length scale, $L_B = (DC_x/N)^{1/2}$, where C_x is the Cox number and D is the molecular diffusivity of temperature, is the same order as L_T near the surface of a mixing layer as well as in the layer interior and in the seasonal thermocline. It is shown, by using the turbulent kinetic energy budget, that L_B/L_T is only weakly dependent on the gradient Richardson number as long as the ratio of eddy viscosity to eddy diffusivity is constant. The temperature variance dissipation rate is compared to the product of the buoyancy frequency and the existing temperature variance. Temperature fluctuations are defined as the temperature difference between the observed temperature profile and the Thorpe profile (the temperature profile which would result if an overturning patch gravitationally collapsed without dissipation). It is shown that the major balance in the temperature variance equation is between the rate at which variance is produced and the rate at which it is dissipated and that the rate of change of temperature variance can be an important modification to this balance only if the variance decays in a time much smaller than a buoyancy period.

1. INTRODUCTION

Theories of turbulent stirring often depend on assumptions about the length scales of turbulent eddies. Early 'mixing length' theories explicitly used the 'size' of turbulent eddies as a fundamental variable. Though our understanding of turbulence has progressed beyond these primitive models, measurements of the length scales of turbulence can provide evidence pertinent to modern theories. *Thorpe* [1977] devised an objective method of estimating a length scale associated with overturning events in a stratified fluid and proposed that the overturning scale should be related to the Ozmidov scale, $L_0 = (\varepsilon/N^3)^{1/2}$, where ε is the kinetic energy dissipation rate and N is the buoyancy frequency. In this report, we test Thorpe's proposal and examine the implications of a relationship between the Thorpe scale and the Ozmidov scale.

The Thorpe Scale

Thorpe's [1977] method for empirically estimating the length scales of turbulent overturning in a stratified turbulent flow is useful for the analysis of vertical density profiles when the flow is homogeneous in the horizontal and density inversions are the result of turbulent stirring. The method consists of rearranging or ordering an observed potential density profile, which may contain inversions, into a stable monotonic profile which contains no inversions. Imagine a density profile as consisting of n samples of density ρ_n, each of which was observed at depth z_n. If the sample at depth z_n must be moved to depth z_m to generate the stable profile, the Thorpe displacement d_n' is $z_m - z_n$ (Figure 1). If each sample density is distinct, the array of Thorpe displacements is unique. When two or more samples have the same density, the set of displacements may depend on the type of ordering used, but in most cases of importance the displacements depend very little on the particular algorithm used. A 'bubble sort' algorithm with ordering beginning at the shallowest depth was used in the following analysis.

Thorpe displacements are useful as a visual aid to define the vertical extent of some mixing events. For example, large disturbances in surface mixing layers often have sharp boundaries and are characterized by a large negative displacement near the top of the disturbance, followed by a mean which slowly becomes more positive (Figure 2, 16–22 m). Displacement fluctuations of a size comparable to the size of the disturbance itself are found in the interior. This is a signature which might be expected for a large overturning eddy: sharp upper and lower boundaries with intense mixing inside. While common in surface layers strongly forced by the wind, these large features are not always found (Figures 3 and 4). When wind forcing is absent, they are not found at all in surface layers. Other features often found in wind-forced surface layers are smaller, some having an 'eddylike' shape similar to the larger disturbances, some a random mix of small-scale fluctuations without sharp boundaries (Figure 3).

The Thorpe scale L_T is defined as the root mean square Thorpe displacement,

$$L_T = \langle d'^2 \rangle^{1/2}$$

where $\langle\ \rangle$ signifies an appropriate averaging process. While the displacement d_n' is not necessarily the distance sample ρ_n actually traveled (eddies are not one-dimensional), The Thorpe scale is proportional to the mean eddy size as long as the mean horizontal density gradient is much smaller than the vertical gradient. It has been suggested that the maximum displacement be used rather than the Thorpe scale for the Ozmidov scale comparison (C. Gibson, private communication, 1981), and all that follows could be cast in these terms. We have chosen to use the Thorpe scale rather than the maximum displacement because we only sample verti-

Paper number 2C1339.
0148-0227/82/002C-1339$05.00

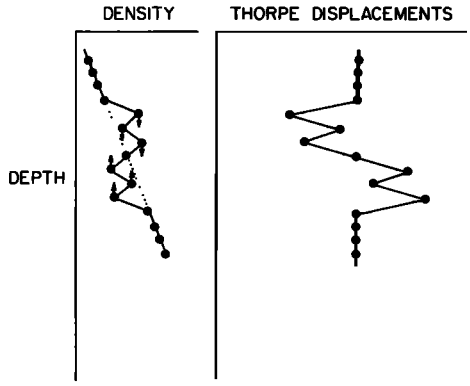

Fig. 1. A hypothetical density profile containing inversions (left) and Thorpe displacements (right) which result from ordering the profile. Arrows near each density sample indicate the direction each sample must move to generate the stable profile. Displacements are negative for downward movement, positive for upward movement. The Thorpe scale L_T is the root mean square displacement. For this example, L_T is 2.7 vertical units and the maximum displacement is 4 units.

cally while the turbulence is three-dimensional; therefore the rms displacement is more likely to be a statistically stable representation of the entire feature.

The Ozmidov Scale

The local turbulent energy budget for a stratified shear flow [cf *Tennekes and Lumley*, 1972] is

$$\frac{1}{2}\frac{\partial}{\partial t}\langle u_i'u_i'\rangle = -\langle u_i'u_j'\rangle\frac{\partial U_i}{\partial x_j} - \varepsilon - (g\rho^{-1})\langle w'\rho'\rangle + \rho^{-1}\left\langle \rho'\frac{\partial}{\partial x_j}(u_j'P')\right\rangle + \frac{\partial}{\partial x_j}\{\nu\langle u_i'\sigma_{ij}\rangle - \rho^{-1}\langle u_j'P'\rangle - U_j\langle u_i'u_i'\rangle\} \quad (1)$$

with

$$\sigma_{ij} = \frac{\partial u_i'}{\partial x_j} + \frac{\partial u_j'}{\partial x_i} \qquad \varepsilon = \frac{1}{2}\nu\langle\sigma_{ij}\sigma_{ji}\rangle$$

where the mean and fluctuating velocities are U_i and u_i', w' is explicitly a vertical velocity fluctuation, g is the acceleration of gravity, ρ and ρ' are the mean and fluctuating density, P' is a pressure fluctuation, and ν is the kinematic viscosity. The physical meaning of each of these terms in an oceanic context has been carefully discussed elsewhere [*Osborn*,

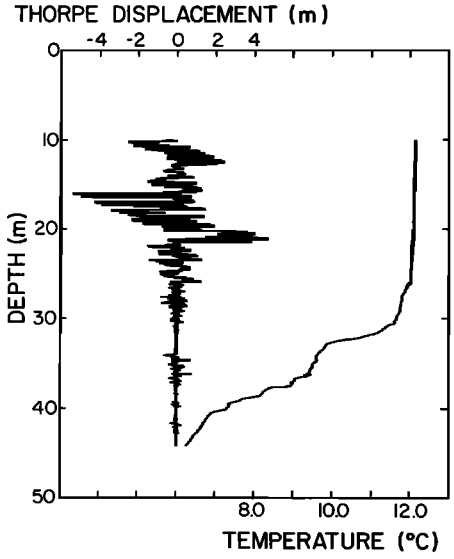

Fig. 2. A temperature profile and the associated Thorpe displacement from cast 2, series B. A large structure extends from 16 to 22 m. The structure has sharp edges and the shape of a reversed z, resembling an overturning eddy. In the interior of the disturbance are fluctuations with displacements nearly as large as the structure itself; the Thorpe scale for this event is 2.0 m, and the size of the structure is 5 m. Other less sharply defined patches can be seen at the base of the surface layer and in the thermocline. The surface wind at the time of the observation was approximately 15 m/s.

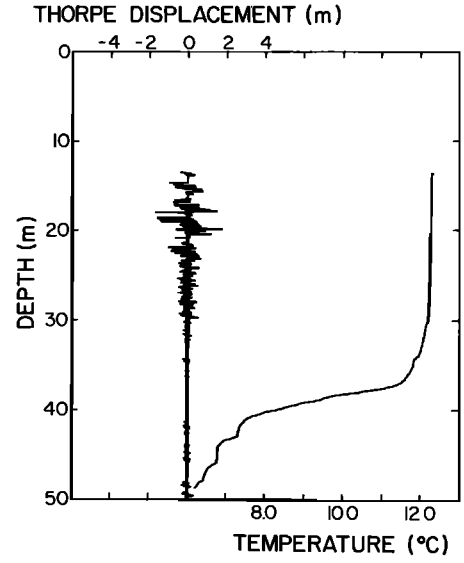

Fig. 3. Temperature and displacement profiles for case 5, series A, when the surface wind was low (3–5 m/s). The displacements for series A were smaller than series B, with very few well-defined 'sharp' features above the thermocline. In the thermocline, there were no distinct differences between series A and B.

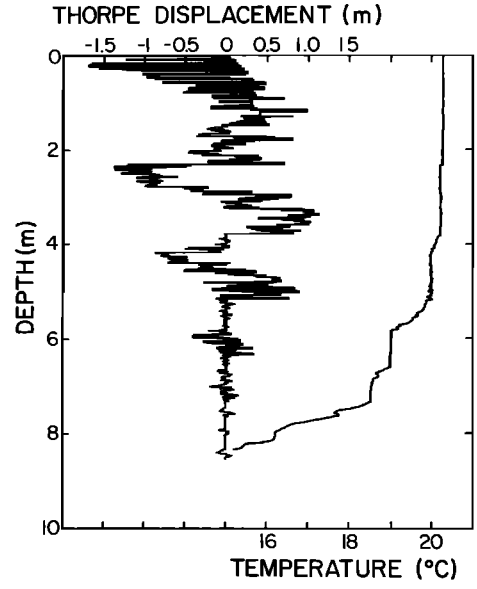

Fig. 4. Temperature and displacement profiles for cast 12 of series C (the freshwater series). Surface winds were steady at 8.5 m/s. Large features with sharp boundaries were again seen above the thermocline (here, at about 8 m depth), and smaller indistinct features were seen in the thermocline.

1980]. The latter three terms are divergences, not sources or sinks, and act only to transport energy from one place to another. Our sampling procedure, described below, minimizes the vertical component of divergences, and there is no reason to believe there is any preferred location in the horizontal. We will neglect these terms. Also ignored will be the fourth term on the right, since as a correlation of a product of three fluctuating quantities, it should be small. Our analysis will be confined to surface layers and seasonal thermoclines where, because the density is determined mainly by temperature, we can use the coefficient of thermal expansion α to approximate density fluctuations as $\rho'\rho^{-1} = -\alpha T'$. As is usually done, we assume that the rate of change of the turbulent kinetic energy is small compared to the source and sink terms (an argument in favor of this assumption appears below). Making the notational simplification that U and u' are the mean and fluctuating velocity in the flow direction, we arrive at

$$-\langle u'w'\rangle \partial U/\partial z = \varepsilon - \alpha g\langle w'T'\rangle . \quad (2)$$

P, the rate of production of turbulent energy, is $-\langle u'w'\rangle \partial U/\partial z$ and the rate of change of potential energy is $-\alpha g\langle w'T'\rangle = B$, the buoyancy flux; (2) may be simply written as $P = \varepsilon + B$.

The size of an eddy may be defined as $l = (-\langle u'w'\rangle)^{1/2}(\partial U/\partial z)^{-1}$. Since $N^2 = -g\rho^{-1}(\partial\rho/\partial z)$ and R_g, the local gradient Richardson number, is $N^2(\partial U/\partial z)^{-2}$, (2) reduces to

$$l = R_g^{3/4}[(\varepsilon + B)/N^3]^{1/2} \quad (3)$$

If we define the local flux Richardson number as $R_f = BP^{-1}$, (3) reduces to

$$L_T = C_l R_g^{3/4}(1 - R_f)^{-1/2} L_O \quad (4)$$

where C_l, an order 1 constant, is the ratio of the overturning scale L_T to the length scale l defined above. We then expect that if R_g and R_f are nearly constant, the Ozmidov scale should be highly correlated with the Thorpe scale.

As pointed out by *Thorpe* [1977], we should not expect (4) to hold except in a strongly averaged sense, because in any single realization the advective terms and rate of change of turbulent kinetic energy may not be negligible. A search for this correlation must involve the examination of many realizations.

2. Measurement Techniques

Three series of microstructure casts through actively mixing surface layers and seasonal thermoclines were used for the comparison. Two of these, series A and B, were collected at Ocean Station P during the MILE experiment (50°N, 145°W, September 1, 1977) and the other, series C, at Green Peter Reservoir (a small impoundment east of Corvallis, Oregon, on July 17, 1981). Though series A and B were taken only 5 hours apart, the surface winds during each series were very different. Prior to series A, winds exceeded 15 m/s for 6 hours. The winds then decreased to less than 5 m/s for 5 hours. In the last hour of this lull the six series A casts were made. The wind then increased to greater than 15 m/s, and during this period the six casts of series B were made. The 16 casts of series C were made during sustained winds of 8.5 m/s.

Series A and B casts were made with a downward profiling instrument, the microstructure profiler (MSP), and series C casts were made with the wave zone profiler (WAZP), an upward profiling instrument. Complete descriptions of the MSP and WAZP have been given elsewhere [*Caldwell and Dillon*, 1981; see also *Caldwell et al.*, 1975]. Each instrument contains fast response thermistors (Thermometrics, model P-85), a pressure sensor, and amplifiers. Two independently amplified signals from the same thermistor are transmitted to shipboard on separate lines of the data link.

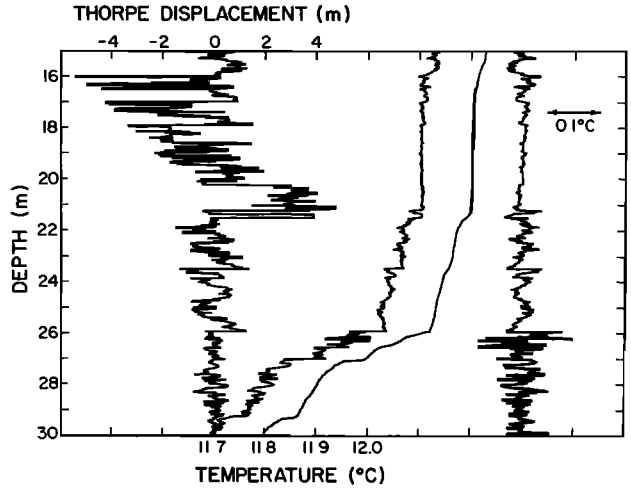

Fig. 5. A detailed illustration (from left to right) of displacements, observed temperature, ordered temperature, and temperature fluctuations (defined as the difference between the ordered and unordered temperature) for the cast of Figure 2. The distinctive sharp edges of the displacement suggest that entrainment is occurring at the edges of the large feature between 16 and 22 m.

The WAZP and MSP have nearly identical sensors and circuitry. The only difference is in the probe body. The MSP is large (~2 m length) while the WAZP is smaller (~1 m length). A nearly constant rate of descent is maintained by four large wings on the MSP, while the WAZP uses a smaller vented drag plate to maintain a nearly constant ascent rate. The MSP is launched from the surface and descends at approximately 10 cm/s. The WAZP quickly descends to a specified depth, where it releases a ballast weight, and then buoyantly ascends at approximately 10 cm/s. The data link is slack during all casts.

3. Buoyancy Frequency Estimates

It is necessary to estimate the buoyancy frequency as well as the dissipation rate to compare the Thorpe and Ozmidov scales. This may pose a problem, as one can imagine a disturbance with negative mean density gradient leading to an imaginary buoyancy frequency. The mean stratification cannot be estimated from a simple average over many casts because of internal wave displacements and distortions. Warping of the density field by internal waves might influence the turbulence, making the instantaneous stratification more important dynamically than a time-averaged mean. The estimate of N must come from each profile rather than from a long-term average.

Another method of estimating N might be to average the density gradient over a length scale much larger than the disturbance size. A defect in this method is that many disturbances are quite localized in the vertical, and a fluctuation in the interior of the disturbance may be quite insensitive to the stratification only a small distance away if the mixing regime is different there. This can be seen in Figure 5,

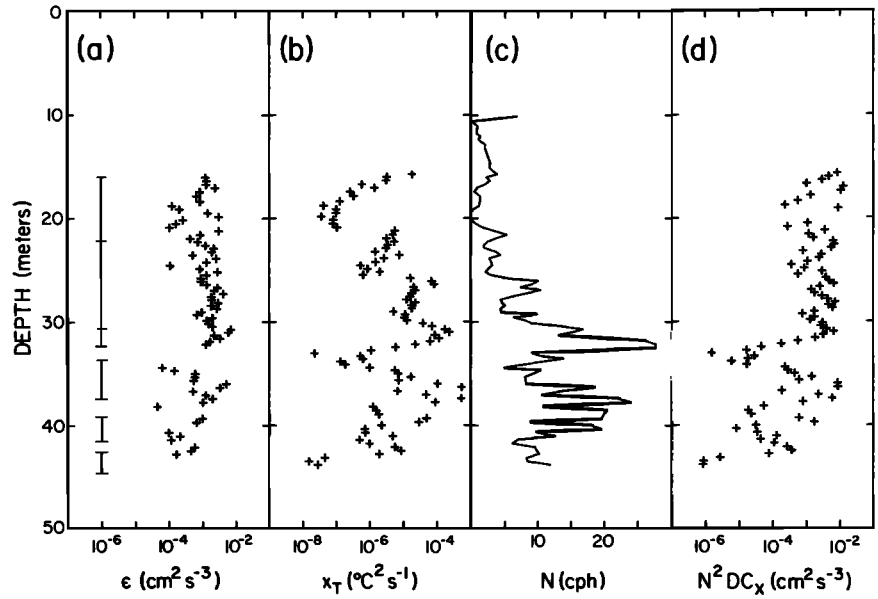

Fig. 6. Estimates of the kinetic energy dissipation rate ε, the temperature variance dissipation rate χ_T, the buoyancy frequency (calculated from the ordered temperature profile over 50-cm segments), and N^2DC_x for the cast of Figure 2. Averaging intervals used to calculate L_T, ε, χ_T, and N for this cast are shown at the left. The intervals were always chosen to completely cover any large distinct features, including a small 25–50 cm interval on either side. N and L_T were calculated from the average of their squares over each interval. The intervals covered all regions except some sections in the thermocline, where no overturns were found, and some sections near the top of the mixing layer, where temperature gradient spectra were not resolved.

where a single well-defined disturbance extends from 16 to 22 m. Here the temperature gradients above and below the disturbance are different from the 'mean' gradient in the interior, and parcels of water above 15 and below 23 m have not been entrained into the interior. Since we require that our estimate of N be representative of the stratification against which the disturbance is actually straining, N must be calculated from the temperature gradient over a depth range just enclosing this particular event, in this case including a small zone (25–50 cm) on either side of the disturbance. Though often envisioned in mixing theories, the case of a constant 'ambient' N applicable to all events in a layer is seldom if ever observed in the field. It may be attainable only in a well-controlled laboratory.

We take the stratification from the ordered profile (Figure 5). The density gradient is first calculated over 50-cm segments for compatability with the dissipation rate estimates and then averaged over the full length of each disturbance. This is similar to using the maximum density difference within each overturn divided by the length of the overturn. (Gradients found in this way are much larger than the gradients found deep within the interior of disturbances, where the stratification may be quite small.) We are then assured of using only the density gradients actually encountered by the fluctuations and the gradients against which each disturbance is actually straining. With this definition, the buoyancy frequency has dynamical significance, since it is related to the change in potential energy that a density fluctuation experiences. Another benefit of using the ordered profile as an estimate of the mean profile is that temperature fluctuations can be unambiguously defined as the difference between the ordered and unordered profiles (Figure 5).

For series A and B we have estimated N in the mixing layer and seasonal thermocline with a relation we found in MILE CTD casts (S. Hayes, personal communication, 1979), $N^2 = 0.01(10.8 + 0.8\ T)\langle \partial T/\partial z \rangle$, where T is in degrees centigrade and $\langle \partial T/\partial z \rangle$ is in degrees per centimeter; $\langle \partial T/\partial z \rangle$ is positive for a stable gradient. This relation was found to hold quite well above 50 m. For the fresh water case (series C) the relation used was $N^2 = 0.0133(T - 4)\langle \partial T/\partial z \rangle$ [*Simons*, 1973].

4. Dissipation Rate Estimates

Dissipation rates were estimated from temperature gradient spectra by the Batchelor wavenumber method [*Dillon and Caldwell*, 1980*a*], an indirect technique which depends on fitting a measured, nondimensionalized spectrum to Batchelor's theoretical form [*Batchelor*, 1959, appendix]. *Oakey* [1982] compared the method with a more direct estimate of the dissipation from an airfoil shear probe and found good agreement. Details of the method have been given elsewhere [*Caldwell and Dillon*, 1981]. In essence, the Batchelor wavenumber method uses the assumption that two competing processes, turbulent stirring and molecular diffusion, determine the large wavenumber temperature gradient spectrum. Turbulent stirring tends to increase temperature gradients and has a time scale $(\nu/\varepsilon)^{1/2}$, while molecular diffusion, which depends strongly on the size of fluctuations and tends to decrease gradients, has a time scale $(Dk_B^2)^{-1}$. Here, D is the molecular diffusivity and k_B, the Batchelor wavenumber, is inversely proportional to the size of the smallest temperature fluctuations. When the time scales for stirring and diffusion are the same, an equilibrium spectrum, the Batchelor spectrum, results. When k_B can be found from the spectrum, the mechanical energy dissipation rate is

$$\varepsilon = \nu D^2 k_B^4 \qquad (5)$$

Spectra were calculated from 50 cm half-overlapping intervals and ε was estimated for each interval (Figure 6).

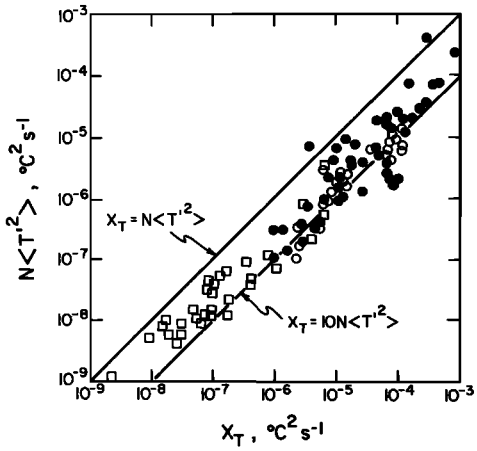

Fig. 7. The temperature variance dissipation rate χ_T plotted versus the product of the buoyancy frequency and an estimate of the temperature variance (the temperature variance is estimated as the mean square difference between the observed and ordered temperature profiles). The correlation is good over nearly six decades. The upper line represents the amount of variance which could be dissipated in time $1/N$ if no new variance were being produced and the lower line the amount of variance which would be dissipated in a time $1/(10N)$. Since the 'standing crop' of variance could be dissipated in an interval much shorter than $1/N$, the individual fluctuations must dissipate before gravitational collapse can occur and additional fluctuations must be continually produced.

The temperature variance equation is [*Tennekes and Lumley*, 1972; *Osborn and Cox*, 1972]

$$\frac{\partial}{\partial t}\langle T'^2\rangle = -2\langle T'u_i'\rangle\langle \partial T/\partial x_i\rangle - 2D\langle(\partial T'/\partial x_i)(\partial T'/\partial x_i)\rangle$$

$$+ \frac{\partial}{\partial x_i}\left[\langle U_i + u_i'\rangle\langle T'^2\rangle + 2D\frac{\partial}{\partial x_i}\langle T'^2\rangle\right] \quad (6)$$

The fourth term on the right represents the molecular diffusion of variance and may be safely neglected. The third term on the right is the divergence of the advective mean and turbulent transport of variance and is neglected as in (2). Assuming that the temperature gradient field is locally isotropic, the rate of dissipation of temperature variance, χ_T, is given by

$$\chi_T = 2D\langle(\partial T'/\partial x_i)(\partial T'/\partial x_i)\rangle = 6D\langle(\partial T'/\partial z)\rangle \quad (7)$$

The latter equality is assigned by assuming local isotropy in the dissipation wavenumber range. By assuming that no mean horizontal temperature gradients exist, (6) reduces to

$$\frac{\partial}{\partial t}\langle T'^2\rangle = -2\langle w'T'\rangle\langle \partial T/\partial z\rangle - \chi_T \quad (8)$$

In addition to the mechanical energy dissipation rate, complete resolution of the smallest temperature gradients allows an estimate of χ_T to be made using (7).

We can make an estimate of the temperature variance $\langle T'^2\rangle$ if we first explicitly define a 'fluctuation.' To do so, consider an isolated mixing event of arbitrary size which initially contains one or more inversions and which has no external energy source. We define the 'adiabatic state' as that state to which the event would gravitationally collapse in an arbitrarily long time if the molecular diffusivity D was identically zero. A one-dimensional estimate of the adiabatic state can be obtained by a Thorpe ordering of the density. It is easily shown that any state of the system which conserves thermal energy while evolving from some initial state will have a potential energy greater than the potential energy of the adiabatic state, the 'ground state' of the system.

We will use the adiabatic state as the state of reference to define temperature fluctuations, that is, a fluctuation at any depth is defined as the difference between the observed temperature and the temperature of the adiabatic profile at that depth. This definition of a fluctuation preserves the important property $\langle T'\rangle = 0$, where $\langle\ \rangle$ is taken to be a vertical average, since no heat is lost in the transformation to the adiabatic state. An important property of the variance admitted by this definition is that for systems having no external energy sources and in which $D = 0$ but $\nu \neq 0$, the variance $\langle T'^2\rangle$ approaches zero when the time becomes large. No other definition of the reference state will have this property. The fluctuation definition is also consistent with the derivation of (6) through (8), since the vertical derivative of the adiabatic profile is much smaller than the derivative of the fluctuations, and the advective terms vanish because the temperature variance is zero on the perimeter of an overturning disturbance.

To calculate $\langle T'^2\rangle$, we in principle imagine a volume average enclosing all of the variance in each disturbance to insure that the divergence of the advective terms in (6) are zero. In practice we use a vertical average covering each disturbance and rely on the randomly selected horizontal position of each cast to provide horizontal averaging when the results of several casts are combined. We define a 'disturbance' as a vertical section containing inversions which seem to be associated by their displacements. In many cases (cf Figure 2, 16–22 m), the disturbance is isolated, and there is little doubt about its vertical extent. In other cases, when the density gradient is stronger (cf Figure 2, 22–30 m), regions containing many small overturns have a vertical extent much larger than the maximum displacement inside the region; for these cases, the vertical averaging interval was always much larger than the maximum displacement.

An assessment of the importance of gravitational collapse in (8) can now be made by comparing χ_T to $\langle T'^2\rangle/t^*$, where t^* is some time scale. Variance relative to the adiabatic state is the precise definition to use in this comparison because it is a measure of the variance which must be destroyed by gravitational restabilization if no potential energy is used to alter the mean state. The comparison of χ_T and $\langle T'^2\rangle/t^*$ is a comparison of two competing processes: the destruction of variance by gravitational restabilization and the destruction of variance by turbulent diffusion.

The variable t^* delimits the time scale over which each process could be dominant and should be chosen to have some relevance to a time scale fundamental to the problem. We choose $t^* = 1/(QN)$, since it is reasonable that the time scale for gravitational collapse may be proportional to the inverse of the buoyancy frequency.

The evidence reveals that χ_T is proportional to and is 3–10 times larger than $N\langle T'^2\rangle$ over nearly six decades (Figure 7). If the rate of change of variance is a dominant term in (8), Q must be in the range 3–10. With few exceptions the time scale for pure decay is smaller than N^{-1} and is always less than the buoyancy period $2\pi/N$. This is a very robust result in which the uncertainty in χ_T (see appendix) is quite negligible. The conclusion one may draw from Figure 7 is straightforward: gravitational decay can be important only if

TABLE 1. Series A, the Low Wind Speed Oceanic Series

Cast	Depth Range, m	Mean Temperature, C	$\langle \partial T/\partial z \rangle$, C/m	N, cph	χ_T, $10^6C^2/s$	$N\langle T'^2 \rangle$, $10^6C^2/s$	C_x	ε, $10^4cm^2/s^3$	N^2DC_x, $10^4cm^2/s^3$	L_T, cm	L_0, cm	L_B, cm	$k_kL_T/3$
A1	12.5–13.8	12.297	0.0015	0.99	0.019	0.0063	32000	0.30	1.4	110	76	160	85
	14.2–19.7	12.281	0.0032	1.48	0.052	0.0099	18000	0.96	1.7	65	75	98	68
	20.0–22.0	12.255	0.0110	2.73	0.048	0.015	1400	0.92	0.45	25	29	20	26
	22.3–23.2	12.236	0.0166	3.35	0.018	0.010	230	0.17	0.11	12	9.1	7.4	8.3
	23.5–25.0	12.194	0.0248	4.09	0.077	0.013	450	1.30	0.32	17	19	9.3	20
	25.3–27.3	12.071	0.0517	5.90	2.9	0.82	3900	6.90	5.8	36	25	23	62
	27.6–31.4	11.159	0.2639	13.17	6.2	0.56	320	7.10	2.3	9.0	7.6	4.4	15
A2	11.6–15.1	12.285	0.0064	2.09	0.083	0.047	7100	0.38	1.3	69	27	52	57
	15.4–20.1	12.269	0.0037	1.58	0.052	0.011	14000	0.76	1.5	100	60	83	100
	20.4–22.8	12.225	0.0170	3.39	0.13	0.056	1600	1.80	0.77	19	29	19	24
	23.2–25.0	12.164	0.0283	4.37	0.16	0.067	720	1.82	0.58	14	13	12	14
	25.3–26.9	12.072	0.0508	5.84	0.45	0.047	618	3.20	0.90	8.3	17	9.2	12
	27.2–28.8	11.931	0.0814	7.38	1.1	0.077	580	4.90	1.3	6.8	15	7.9	11
	29.1–30.4	11.601	0.2107	11.82	1.9	0.13	150	2.70	0.89	4.4	5.5	3.2	6.0
	33.3–34.2	8.906	0.4625	16.55	4.0	0.22	66	2.10	0.77	4.2	2.9	1.8	5.4
	37.1–38.6	6.934	0.1548	9.13	0.17	0.013	25	0.17	0.088	3.1	2.1	1.5	2.1
A3	15.8–19.7	12.279	0.0023	1.25	0.081	0.033	55000	0.81	3.6	190	89	190	190
	25.3–31.2	12.135	0.0200	3.67	9.5	0.015	850	1.10	0.49	14	20	14	15
	31.5–37.6	11.405	0.1320	9.35	2.9	0.19	590	5.50	2.2	6.1	11	7.1	9.8
A4	12.8–15.2	12.280	0.0037	1.58	0.0022	0.0012	580	0.21	0.062	29	32	17	20
	15.6–17.8	12.267	0.0042	1.69	0.015	0.0074	3000	7.5	0.36	48	17	38	27
	18.1–19.8	12.257	0.0053	1.89	0.031	0.0091	3900	0.77	0.59	37	46	40	37
	20.2–25.4	12.237	0.0039	1.63	0.027	0.0045	6400	0.82	0.72	67	60	56	67
A5	25.6–30.9	12.153	0.0180	3.49	0.091	0.013	1000	0.92	0.52	18	20	15	18
	31.2–33.0	12.047	0.0519	5.91	0.18	0.023	240	1.90	0.36	5.9	13	5.7	7.3
	33.6–36.5	11.609	0.1355	9.49	0.80	0.12	160	2.30	0.60	4.0	7.1	3.6	5.2
	40.7–42.7	7.344	0.2104	10.79	0.41	0.046	33	0.79	0.16	4.5	3.4	1.6	4.4
	44.1–45.7	6.801	0.0261	3.73	0.032	0.0052	170	0.29	0.099	6.3	10	6.0	4.9
A6	19.1–20.7	12.259	0.0035	1.53	0.0091	0.0032	2700	0.12	0.27	42	25	38	26
	21.0–23.6	12.242	0.0064	2.08	0.010	0.0042	910	0.44	0.17	34	30	19	29
	23.9–27.1	12.212	0.0088	2.44	0.0090	0.0055	410	0.27	0.10	20	19	12	15
	27.4–36.5	11.158	0.1169	8.79	6.5	0.35	1700	6.80	5.6	7.5	14	12	13

The χ_T is the rate of dissipation of temperature variance, and $N\langle T'^2 \rangle$ is the product of the bouyancy frequency and the temperature variance of the observed state relative to the adiabatic state (the state of minimum potential energy which conserves thermal energy). The ratio of χ_T to $N\langle T'^2 \rangle$ is an estimate of the time, in units of $1/N$, in which the variance would dissipate if the variance production were negligible. The $k_kL_T/3$, one third the product of the Kolomogrov wavenumber and the Thorpe scale, is an estimate of the size of the turbulent cascade wavenumber range.

it occurs within a small fraction of one buoyancy period. While some contend that the variance in an isolated patch having no external energy sources may persist for much longer than $(2\pi/N)$ [*Gibson*, 1982], it is not reasonable to expect the variance in a patch will decay much faster than $1/N$.

We conclude that the rate of decay of temperature variance in most cases cannot be an important term in (8) and assume that $-\langle w'T' \rangle$ must be greater than 0, a source of temperature variance, not a sink. This results in the familiar Osborn-Cox estimate of the heat flux,

$$-\langle w'T' \rangle = \tfrac{1}{2}\chi_T\langle \partial T/\partial z \rangle^{-1} = DC_x\langle \partial T/\partial z \rangle \qquad (9)$$

where C_x is the Cox number $3\langle(\partial T'/\partial z)^2\rangle\langle \partial T/\partial z \rangle^{-2}$. Individual fluctuations of temperature are quickly extinguished because χ_T is large, but fluctuations are constantly being replenished by $-\langle w'T' \rangle\langle \partial T/\partial z \rangle$, and the variance cannot change rapidly. If the time scale for the restratification processes was known, we could in principle correct for the time rate of change of variance as gravitational collapse occurs. Any correction to (9) would be entirely negligible if *Gibson* [1982] is correct in asserting that the typical lifetime of a decaying patch is many buoyancy periods. If however, the gravitational decay has a time scale as small as $1/N$, the decay correction might sometimes be important. All we can say at present is that gravitational restratification effects are almost always small. If the rate of decay of temperature variance is negligible in (8), we can safely assume that the rate of decay of kinetic energy in (1) is also negligible, since the Prandtl number is greater than 1 for water.

5. The Comparison

It is important to include as much of the water column as possible in the Thorpe scale calculation, for if an observation does not include the full extent of a disturbance, displacements may be underestimated. For the MILE data of series A and B, only sections below 10 m depth were analyzed because of the possibility of interference from the ship. For the lake casts the profiler was launched from a shallow draft anchored boat and typically reached the surface 10–30 m from the boat. Data were useful to within a few centimeters of the surface.

A constraint on the comparison is that both the Thorpe scale and the dissipation rate must be resolved in regions where the comparison is made. The averaging length must be long enough to include all of a distinct disturbance, yet short enough that conditions do not change greatly. A fixed averaging length is not appropriate. We averaged over the entire extent of a disturbance whenever a distinct structure (cf Figures 5 and 6) was seen. When a distinct structure

could not be found, an averaging interval was chosen to minimize changes in the individual subsamples of N, ε, and L_T within an average; these intervals, occurring in the lower part of the mixing layer and in the seasonal thermocline, were often associated with large N, small ε, and small L_T.

Some of the data were excluded from the analysis. These were segments in which (1) the dissipation rate was so large that the gradient spectrum could not be resolved (these segments were typically near the surface), (2) a distinct microstructure peak was not found in the gradient spectrum (these segments were usually found in highly stratified regions and had a very small or zero Thorpe scale), or (3) a large but 'incomplete' eddy was found (these were segments in the MILE casts where a recognizable eddy protruded above 10 m; cf Figure 2, 10–13 m).

We first calculated ε, N, and L_T over 50-cm half-overlapping segments. When a recognizable eddy was seen in plots of displacement, ε, N^2, and L_T^2 were averaged over the eddy with care taken to insure that the segments completely covered the eddy. Values of N and L_T were found from the average of their squares; a similar procedure was used for averaging intervals where no distinct structure could be found. In all cases the averaging length was larger than the maximum displacement in the average.

The Thorpe scale and the Ozmidov scale are nearly equal for both series A and B casts (Table 1). A regression of the form $L_0 = aL_T^n$ on series B casts resulted in $n = 0.95$ with a regression coefficient of 0.98 (Figure 8). Since n was not much different from 1, we evaluated a from the mean ratio: $a = \langle L_0/L_T \rangle = 0.8$.

The above test was applied to series B, where because of the more strongly driven turbulence, (3) and (4) were expected to hold better than in the low wind speed, weakly driven, and possibly decaying case of series A. For series A, $\langle L_0/L_T \rangle = 0.9$, 11% higher than for series B. If the variance is from a Gaussian distribution, a value larger than 0.9 would be observed with a 25% probability from the population of series B (Figure 9). We conclude that there is little difference between the populations of series A and B.

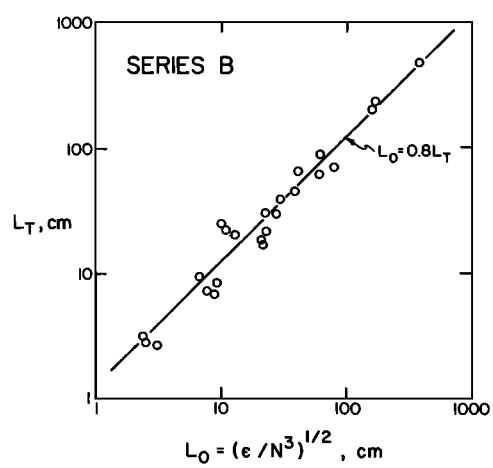

Fig. 8. The Thorpe scale plotted against the Ozmidov scale for series B, the high-wind oceanic casts. A striking correlation is seen over nearly three decades. The line drawn represents the equation $L_0 = 0.8\ L_T$. A linear relation is expected if the gradient and flux Richardson numbers are both constant.

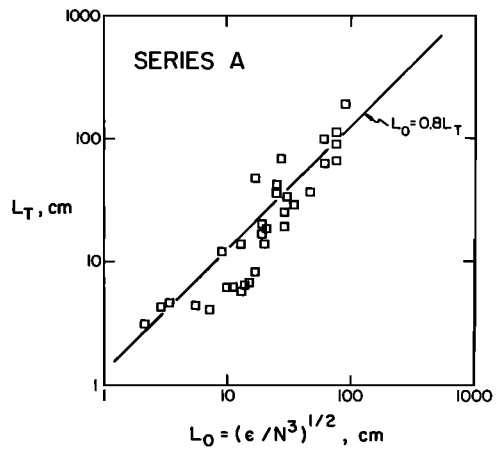

Fig. 9. The Thorpe scale plotted against the Ozmidov scale for series A, the low-wind oceanic casts. More scatter is present than in Figure 8, but the correlation is still represented well by the line $L_0 = 0.8\ L_T$.

A constant proportionality between L_0 and L_T cannot be expected to hold in regions where the Richardson numbers are not constant. The near-surface regions sampled in series C provide just such a counterexample to series A and B, since we must expect R_g to be smaller very near the surface than deep within a mixing layer. Our estimate of the buoyancy flux, $B = N^2DC_x$, is much smaller than ε near the surface in series C, while B and ε are of the same order in all of series A and B, as well as at the mixing layer base and in the thermocline in series C (see tables). L_0 and L_T are of the same order for $L_0 < 30$ cm in the series C casts, but L_0 becomes significantly larger than L_T for $L_0 > 30$ cm (Figure 10). These large values of L_0 are all from the upper 4 m, where B/ε is smaller than elsewhere.

As a guide to understanding the near-surface observations, we note that the few measurements made in the atmospheric boundary layer in stable stratification indicate that the ratio of gradient to flux Richardson number (or, equivalently, the ratio of eddy viscosity to eddy diffusivity)

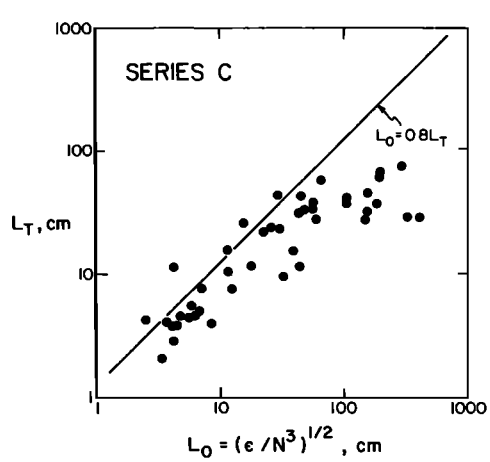

Fig. 10. The Thorpe scale plotted against the Ozmidov scale for the lake casts, series C. The ratio of the Ozmidov scale to the Thorpe scale is similar to the oceanic casts for points originating at the base of the mixing layer and in the thermocline, but much larger for many points from the near-surface zone. The difference is attributed to the decreasing gradient and flux Richardson numbers in the near-surface zone.

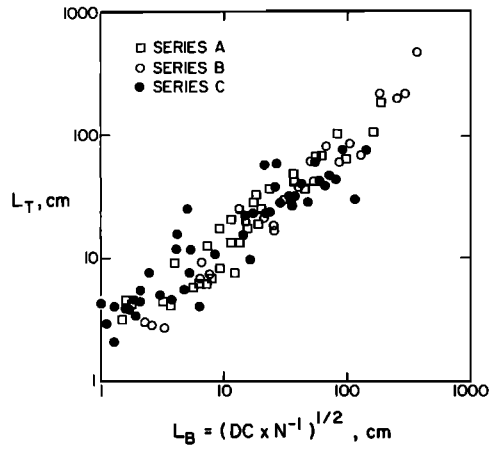

Fig. 11. The Thorpe scale plotted against $L_B = (DC_X/N)^{1/2}$ for all data. The correlation is good for all regions observed, including thermoclines, mixing layer interiors, and the near-surface zone. The ratio of L_B/L_T is expected to depend on the 0.25 power of the gradient Richardson number and hence is more nearly constant than L_0/L_T when the Richardson number decreases in the near-surface zone.

is independent of the bulk stratification (cf *Businger et al.* [1971]; note, however, that the range of gradient Richardson number in these observations is not large). Defining $L_B = (B/N^3)^{1/2}$ and rewriting (3) as

$$L_T = C_l R_g^{1/4}(R_g/R_f)^{1/2} L_B \qquad (10)$$

we expect that L_B/L_T should be constant in a wider variety of instances than L_0/L_T, since L_B/L_T is only weakly dependent on R_g if R_g/R_f is nearly constant. The near-surface differences seen when comparing L_0 and L_T (Figure 10) are not present when L_B and L_T are compared (Figure 11). Although the scatter is large, the ratio L_B/L_T appears to have the same mean value in thermoclines, in mixing layer interiors subject to various degrees of surface forcing, and in the near-surface zone.

The ratio L_B/L_T for all the data is 0.93. The scatter about this ratio, measured as the standard deviation of $(1 - 0.93\ L_B/L_T)$, is 0.3 for series A and B together and 0.6 for series C alone. The larger scatter in series C is in large part due to smaller vertical averaging intervals than in series A and B. The mean size of interval for series A and B was 3.5 m but only 1.6 m for series C. A typical point from series A or B represents twice as long a sample as a typical point from series C.

6. Discussion

Deep in the interior of actively mixing surface layers and in the seasonal thermoclines we have seen, the ratio of the Ozmidov scale to the Thorpe scale was remarkably constant. The near-surface series C measurements make it clear that this relation does not always hold. We interpret the near surface measurements as indicating a change in both the flux and gradient Richardson numbers. The ratio of buoyancy flux to energy dissipation was smaller near the surface than in the mixing layer interior, indicating a smaller flux Richardson number. We expect the gradient Richardson number to be smaller in this region since, near the surface, shears increase while density gradients decrease.

In all observed circumstances a constant of proportionality was found relating $(B/N^3)^{1/2}$ and L_T. A relationship might be caused by gravitational collapse if the decay was an exponential function of time, but we have shown that the

TABLE 2. Series B, the High Wind Speed Oceanic Series

Cast	Depth Range, m	Mean Temperature, C	$\langle \partial T/\partial z \rangle$, C/m	N, cph	χ_T, $10^6C^2/s$	$N\langle T'^2 \rangle$, $10^6C^2/s$	C_x	ε, $10^4cm^2/s^3$	N^2DC_x, $10^4cm^2/s^3$	L_T, cm	L_0, cm	L_B, cm	$K_kL_T/3$
B1	26.3–31.5	11.845	0.0449	5.48	11	1.7	19000	15	24	65	41	53	130
	*31.8–33.8	11.481	0.1723	10.67	72	4.2	8700	32	42	17	22	26	42
	*34.1–35.8	11.177	0.1474	9.79	89	9.4	15000	39	60	30	28	35	79
	48.0–49.5	5.719	0.0794	6.34	2.5	0.35	1400	1.3	2.4	25	10	13	28
B2	15.7–21.6	12.089	0.0069	2.16	2.3	0.10	170000	14	33	200	160	250	420
	21.9–30.1	11.654	0.0525	5.91	16	1.5	20000	17	30	43	39	52	92
	*30.4–32.1	10.591	0.6045	19.73	110	6.0	1100	34	18	8.4	9.1	6.7	21
	33.8–37.4	8.878	0.2422	12.02	108	14	6600	12	41	23	11	21	44
	39.3–39.7	7.341	0.4189	15.19	40	6.8	800	8.2	7.9	9.3	6.6	6.5	16
	42.1–42.8	6.498	0.1865	9.91	5.4	0.33	560	4.0	2.3	6.6	8.8	6.7	9.8
B3	14.6–22.8	11.986	0.0173	3.41	6.0	0.30	71000	13	35	70	80	130	140
	*23.1–27.5	11.732	0.0553	6.07	74	8.2	87000	44	140	89	61	110	240
	*27.9–32.8	10.928	0.1584	10.16	80	11	11000	31	50	30	23	30	76
B4	*10.8–22.8	12.095	0.0059	1.98	2.7	0.19	280000	60	47	480	380	340	1400
	23.1–27.8	11.357	0.1463	9.85	61	5.4	10000	28	42	22	23	29	53
	28.2–32.6	10.275	0.2406	12.38	15	2.5	890	5.9	5.8	7.2	7.6	7.6	12
B5	*21.5–27.2	11.961	0.0136	3.01	6.3	0.98	120000	44	47	230	170	180	630
	*27.6–29.4	11.766	0.1105	8.57	61	5.3	18000	30	56	39	30	41	95
	*29.8–31.8	11.372	0.2049	11.59	110	5.7	9500	35	54	18	21	26	47
	32.5–33.3	10.707	0.3496	14.97	7.1	0.88	210	1.7	2.0	2.6	3.1	3.3	3.1
B6	19.5–24.1	11.978	0.0312	4.57	12	2.4	44000	19	39	62	62	88	140
	24.4–30.9	11.130	0.1282	9.18	12	2.0	2600	7.0	9.4	20	13	15	34
	33.4–34.9	9.424	0.4533	16.62	8.1	0.13	140	1.4	1.7	2.8	2.4	2.6	3.2
	39.3–41.1	7.346	0.1463	8.98	0.34	0.0094	57	0.22	0.20	3.0	2.4	2.3	2.1

The rates of dissipation of kinetic energy and temperature variation, as well as the Thorpe scales, are much larger in the mixing layer than for series A, even though series B was observed only a few hours after series A. In the thermocline (approximately 30 m and below), series A and B do not differ much.

* Marginally resolved. All other entries are well resolved.

TABLE 3. Series C, the Series From a Freshwater Lake

Cast	Depth Range, m	Mean Temperature, C	$\langle \partial T/\partial z \rangle$, C/m	N, cph	χ_T, $10^6C^2/s$	$N\langle T'^2 \rangle$, $10^6C^2/s$	C_x	ε, $10^4cm^2/s^3$	N^2DC_x, $10^4cm^2/s^3$	L_T, cm	L_0, cm	L_B, cm	$K_kL_T/3$
C1	8.3–5.8	19.182	0.7521	21.71	12	1.0	78	18	1.6	4.6	5.8	1.7	9.9
	4.6–3.8	20.282	0.3744	16.19	20	7.6	507	53	5.7	26	15	5.0	74
C2	9.5–7.2	18.449	1.4138	27.91	49	5.0	88	21	2.9	3.9	4.2	1.6	8.8
	6.8–4.5	20.232	0.6118	20.28	12	0.022	110	15	2.0	5.5	5.9	2.1	12
	4.1–2.8	20.350	0.0406	5.38	11	0.98	24000	97	30	42	110	60	140
	2.2–1.1	20.377	0.0166	3.44	1.4	0.25	19000	72	9.5	37	180	66	110
C4	8.4–6.9	18.578	1.0410	24.95	16	9.2	53	11	1.4	4.0	3.7	1.3	7.7
	6.6–3.5	20.264	0.4847	18.09	40	7.7	610	50	8.5	7.5	12.6	5.2	21
C5	*5.8–4.0	20.137	0.3018	14.49	130	13	5000	160	44	9.6	32	17	36
	3.7–2.8	20.328	0.0717	7.14	2.7	0.37	1900	28	4.0	16	38	14	37
	*1.5–1.0	20.359	0.0181	3.59	0.96	0.11	10000	270	5.8	29	330	48	122
C6	9.8–8.1	16.527	1.3822	26.25	293	410	550	18	16	12	4.4	4.1	26
	7.7–5.3	19.607	1.0974	26.08	170	20	500	39	15	4.6	6.4	3.9	12
	*4.1–3.3	20.247	0.1760	11.14	100	20	12000	260	62	28	59	29	120
	*2.9–1.9	20.342	0.0451	5.67	7.5	2.2	13000	110	18	40	110	43	140
	1.6–0.5	20.345	0.0107	2.76	0.93	0.33	29000	38	9.5	76	190	92	200
C7	7.8–6.2	18.952	0.7936	22.25	3.6	7.4	20	3.8	0.43	4.2	2.5	1.0	6.2
	5.4–4.6	19.540	0.2934	14.08	92	2.6	3800	79	32	22	23	15	71
C8	7.1–5.2	19.439	0.4154	16.51	71	14	1500	33	17	11	12	8.4	27
	*3.7–2.6	20.300	0.1655	10.82	120	20	16000	120	78	31	43	34	110
	*2.1–1.2	20.321	0.0139	3.15	2.9	0.19	53000	270	22	29	405	120	120
C10	*3.7–1.9	20.299	0.0273	4.40	6.1	0.97	29000	110	24	46	160	73	159
C11	11.2–10.4	13.496	0.4792	13.92	10	6.7	160	6.8	1.3	5.0	6.9	3.0	8.5
	7.3–5.3	19.615	1.0178	25.47	11	1.6	38	16	1.1	2.9	4.2	1.1	6.1
	*5.0–2.9	20.226	0.1920	11.61	64	16	6200	170	36	44	45	21	166
	*2.5–1.1	20.276	0.0125	2.98	3.4	0.72	77000	120	29	75	293	144	262
C12	8.3–6.7	18.793	1.9322	33.13	155	75	148	65	6.9	4.5	5.8	1.9	14
	6.4–5.3	19.854	0.6872	21.53	63	21	475	72	9.4	16	12	4.2	49
	*4.4–3.5	20.250	0.1591	10.58	46	19	6400	260	31	58	65	22	250
	*3.1–1.7	20.289	0.0352	5.00	8.8	4.2	25000	250	27	61	193	64	250
C13	7.3–5.5	19.274	1.2448	27.87	26	3.8	61	12	2.0	2.1	3.2	1.3	4.2
	*5.0–3.7	20.128	0.3991	16.64	280	36	6200	220	74	24	30	17	96
	*3.3–2.2	20.215	0.0335	4.87	2.7	1.3	8500	150	8.6	32	160	38	120
C14	*6.7–4.5	20.016	0.5982	19.89	72	22	720	130	12	12	18	5.4	42
	*5.0–2.6	20.198	0.2245	12.49	85	16	6000	220	40	34	47	20	140
C15	*11.3–9.0	14.271	0.5254	14.87	810	240	11000	220	99	24	35	24	97
	8.6–4.9	19.890	1.3718	28.22	67	38	130	38	4.3	3.4	5.6	1.9	8.9
	*4.5–2.4	20.185	0.0924	8.06	17	0.040	7100	310	20	58	110	27	260
C16	4.7–2.2	20.113	0.0963	8.20	18	3.7	7100	92	20	38	56	26	120
	*1.4–1.1	20.129	0.0149	3.24	1.6	0.013	26000	150	12	44	290	81	164
C17	9.8–8.7	14.547	0.8809	19.61	220	30	1000	29	17	4.0	8.5	6.4	10
	9.5–9.1	14.378	1.4680	25.29	440	76	730	58	20	5.6	8.2	4.8	16
	*5.1–3.8	20.091	0.3984	16.57	370	71	8400	210	98	22	30	20	90
C18	13.5–12.7	12.079	0.4378	12.34	5.4	0.040	100	4.8	0.65	7.6	7.0	2.5	12
	7.4–4.7	19.986	1.5193	30.17	70	2.5	107	28	4.2	3.8	4.4	1.7	9.3
	*4.2–1.5	20.178	0.0420	5.43	4.4	0.032	8900	180	11	27	150	36	110

The Thorpe scales here were generally smaller and N larger than for series A and B. The ratio of the Ozmidov scale to the Thorpe scale was much larger near the surface of the lake than in any of the thermocline or mixing layer interior observations, but L_B/L_T was more nearly constant everywhere. In only two instances (C6, 9.8–8.1 m and C7, 7.8–6.2 m) was $N\langle T'^2 \rangle$ found to be larger than χ_T, indicating that the gravitational decay of an event can be the dominant term in the temperature variance equation only if the time scale for decay is a small fraction of the bouyancy period.

*As in Table 2.

time scale would have to be unreasonably small for decay to be a dominant process. The relationship must therefore exist because $-\alpha g\langle w'T' \rangle$ is proportional to N^2DC_x.

In order for three-dimensional turbulence to exist, there must be a separation of the production and dissipation length scales. The smallest length scale of velocity fluctuations may be estimated as $3(\nu^3/\varepsilon)^{1/4}$, using the inverse of the wavenumber at which the 'universal' shear spectrum falls to half of its peak value [*Oakey*, 1982]. We expect the production length scale to be of order L_T. The dynamic range of the velocity spectrum in which a turbulent cascade might be expected may then be estimated as

$$r = \tfrac{1}{3}(\varepsilon/\nu^3)^{1/4}L_T$$

For the series A and B, $\langle r \rangle = 12$ in the thermocline. In the mixing layer, $\langle r \rangle = 40$ for series A and $\langle r \rangle = 200$ for series B. For series C, $\langle r \rangle = 15$ in the thermocline region and 120 in the mixing layer. The 'cascade' wavenumber range thus has an extent of about a decade in the thermoclines, 1.5 to 2 decades in the mixing layers of series A and C, and more than 2 decades in the strongly driven mixing layer of series B. *Gibson* [1982] argues that the wavelength of the smallest overturning eddy is $15(\varepsilon/\nu^3)^{1/4}$, implying that the minimum dynamic range is of order 10. As might be expected because of sampling error, individual values of r smaller than 10 were sometimes seen (see tables), but the average value of r in highly stratified regions seems to bear out Gibson's estimate.

Because eddies lose directional information as the spectral

cascade proceeds, isotropy on the smallest scales is dependent on the extent of the cascade range of wavenumbers. A sufficiently large spectral range is necessary for isotropy on the smallest scales. We cannot quantitatively predict how isotropy depends on the extent of the cascade wavenumber range, but we expect that the turbulence in all of the mixing layers studied was locally isotropic in the dissipation wavenumber range. Anisotropies may or may not be important in the thermocline examples.

Stillinger [1981] measured overturning length scales in a stratified water tunnel, using the prescription $2\rho_{rms}'\langle\delta\rho/\delta z\rangle$ (a quantity identical to $2L_T$ for a well-defined constant mean density gradient; below, we will use his result expressed in terms of L_T). Behavior consistent with unstratified turbulence was observed as long as $L_0 > 1.4\ L_T$, and stratification was found to be important only if $L_0 < 1.4\ L_T$. *Gibson* [1982] uses Stillinger's results to deduce that $L_0 > 1.4\ L_T$ in order for the turbulence to be 'active' (presumably, 'active turbulence' is identical to turbulence unaffected by stratification). If $L_0 < 1.4\ L_T$, as we observe in all except the near-surface zone, Gibson concludes the turbulence is 'fossil.'

If the overturns we observe are not actively producing fluctuations but are instead relics of previously active mixing events, the time scale of gravitational collapse cannot be longer than $1/N$ and certainly not as long as many days, as asserted by *Gibson* [1982] for some microstructure overturns. We concur with *Stillinger* [1981] in finding that stratification is important for the observed ratio of L_0 to L_T. We do not find instances where the rate of production of temperature fluctuation is negligible. Stillinger, in contrast, finds regions far downstream from the stirring grid where density fluctuations persist and $\langle\rho'w'\rangle$ is negligibly small. Perhaps oceanic turbulence cannot be accurately modeled as grid turbulence in this important respect.

We prefer to term the overturns simply as examples of turbulence in a stratified fluid rather than as fossil turbulence because the fossil terminology implies very specifically that most of the dissipation of energy and temperature variance occurred at some time previous to the observation, and we have no means of determining the state of an event prior to when it was observed. *Gibson* [1982] proclaims that

> The fossil temperature turbulence lifetime presumably ends when the last zero-gradient point produced by the initial active turbulence event is annihilated by molecular diffusion.

The disappearance of 'zero gradient points' must be coincident with the disappearance of density inversions, and we have shown that the mean lifetime of individual fluctuations must be shorter than $1/N$. The events seen must therefore draw energy from some source or rapidly disappear. Since similar mixing events are seen in each cast of every series of casts and each series lasted for considerably longer than $1/N$, it would be a remarkable coincidence if all the overturning events were decaying. We have shown that the relation of the Thorpe scales to length scales based on the small-scale dynamics are understandable in terms of the turbulence energy budget. We need not invoke the ideas of fossil turbulence in order to understand the length scales of overturning events.

Whatever the state of the turbulence beneath the surface zone may be, the length scales of vertical overturning events appear to obey consistent rules and are closely tied to the dissipation scale variables. Perhaps some of the overturns are slowly decaying, some are in a true steady state, and some are growing, yet all the large overturning scales can be closely related to the microscale turbulence. An equilibrium may exist between inertial and gravitational forces during most of the life of an overturning event, with an initial instability very quickly growing to a size large enough that its internal dynamics are constrained by gravitational forces. Most of the kinetic energy and temperature variance dissipated by an event may be done long after the initial instability occurred.

We interpret the results of section 4 to be consistent with conventional ideas of steady state turbulence produced by local shear instabilities. The buoyancy flux and mechanical energy dissipation act as a sink in (1) and are balanced by the local shear production. Temperature-velocity correlations, which are a sink of mechanical energy in (1), are a source of temperature variance in (8). The rate of creation of temperature variance is balanced by its rate of dissipation. The rate of decay of temperature variance is at most a small correction to this balance in the usual circumstances.

7. Conclusions

1. The rate of decay of temperature variance due to gravitational collapse can be an important term in the temperature variance budget only if the time scale for collapse is much smaller than a buoyancy period. This suggests that the major balance in the temperature variance equation is between the rate of turbulent production of temperature variance and the rate of turbulence dissipation.

2. Deep in the interior of wind-forced surface mixing layers and in the seasonal thermocline, the Thorpe scale is of the same order as the Ozmidov scale. This suggests that in a wide variety of conditions the gradient and flux Richardson numbers may be nearly constant.

3. Near the surface of a wind-forced mixing layer, the Ozmidov scale was significantly larger than the Thorpe scale. The ratio of N^2DC_x to the kinetic energy dissipation rate, as estimated by the Batchelor wavenumber method, also decreases near the surface. This is consistent with a decrease in both flux and gradient Richardson numbers as the surface is approached. The value of the Richardson numbers may therefore be constant only in weakly forced mixing regimes, and some caution should be used in assuming Richardson number constancy.

4. Near the surface of mixing layers, as well as deeper within the layer and in seasonal thermoclines, the Thorpe scale is of the same order as $(DC_x/N)^{1/2}$. This suggests that the ratio of gradient to flux Richardson number and hence the ratio of eddy viscosity to eddy diffusivity might on average not be a strong function of the strength or type of mixing regime. It is suspected that the observed scatter in the ratio of $(DC_x/N)^{1/2}$ to the Thorpe scale is purely random statistical variability. Whether or not this variability expresses a random variability in the gradient to flux Richardson number ratio remains to be determined.

Appendix: Some Details of the Analysis

Two signals from the same sensor were redundantly amplified and sent through the data link on independent conductors. Two channels of the temperature signal, as well as the pressure signal, were recorded. The temperature signal was also sent through an analog differentiator and low-pass filter with a cutoff frequency f_c and recorded. For series

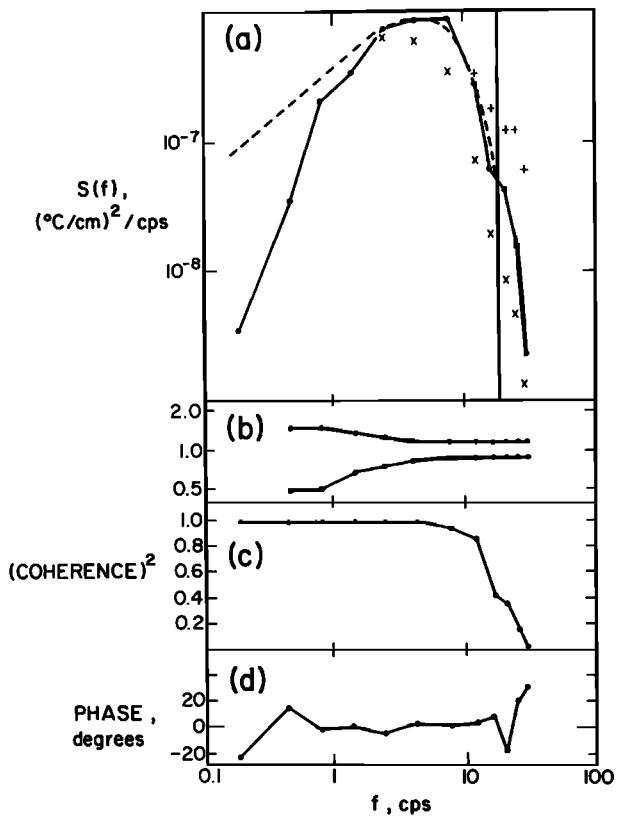

Fig. A1. (*a*) In-phase power frequency spectrum, corrected for sensor frequency response, for a 512-point segment starting at 19.3 m depth, series B, cast 2 (solid circles joined with solid line). For this segment, $\varepsilon = 2.1 \times 10^{-3}$ cm^2/s^3 and $\chi_T = 7.0 \times 10^{-8}$ C^2/s. The dotted line is the Batchelor spectrum for the above values of the kinetic energy and temperature variance dissipation rates. The single spectrum uncorrected for sensor frequency responses (crosses) and the corrected single spectrum (plus signs) are shown when they differ from the in-phase power. Points to the right of the vertical line are noise contaminated and are discarded. (*b*) A white noise estimate of the 63% confidence level for the spectrum, $1 + \sqrt{n}$, where n is twice the number of frequency bands in the spectral estimate. Relative vertical scale is the same as above. (*c*) The coherence and (*d*) the phase of the two redundant channels show that frequencies higher than 20 cps are noise contaminated in this example.

A and B, f_c was set at 30 Hz, and for series C, f_c was 40 Hz.

Data records were broken into segments of 512 points, representing approximatly 50 cm of the water column. A Gaussian window was applied to the temperature derivative signal, and the variance was corrected to its unwindowed value. A fast Fourier transform was then applied to each of the redundantly amplified temperature gradient channels. The power spectrum was band-averaged, and the coherence, phase, and in-phase power [*Caldwell et al.*, 1968] was calculated from the two channels (Figure A1). The highest frequencies were corrected for filter rolloff when necessary. No frequencies higher than 30 Hz were used in this study.

A frequency response correction function,

$$R(f) = 1 + 0.0264\, f^2 - 2.19 \times 10^{-6}\, f^4 + 3.26 \times 10^{-8}\, f^6$$

was applied to the spectra. This correction was found by passing a P-85 thermistor through a thin laminar jet [*Dillon and Caldwell*, 1980*a*; *Caldwell and Dillon*, 1981]. $R(f)$ was originally determined using a representative thermistor from the MILE experiment sensors (series A and B). Later tests with other sensors have shown that $R(f)$ flattens the spectrum in the 7–30-Hz frequency band to better than 20% for all thermistors examined (including the sensor used for the series C casts).

The response in the 0–7-Hz band is more difficult to determine than at high frequencies [cf *Gregg and Meagher*, 1980]. At low frequencies, $R(f)$ may overcorrect, leading to a flat, systematic overcorrection at high frequencies. An upper bound on the error is 30%, and we consider a 30% uncertainty acceptable.

The frequency beyond which the signal becomes significantly smaller than noise, f', is determined by an examination of the coherence and phase of the redundantly amplified temperature gradient channels. When the coherence begins to fall rapidly and the phase oscillates wildly, noise is dominant; nothing can be learned from higher frequencies. We normally use the criteria that the coherence must be above 0.5 and the phase no larger than 10 degrees for a spectral band to be used. Most of the noise originates in the amplifiers of the probe instead of in the sensor itself. When the coherence and phase criteria are met, the in-phase power can be used to remove most of the noise, since the signals on the redundantly amplified channels are coherent, while the noise fluctuations are incoherent. The coherence and phase criteria above were found by examining spectra from very 'quiet' regions and spectra from casts which used a fixed resistor in place of the sensor. Although the in-phase power calculation can remove incoherent noise even when the coherence is less than 0.5, noise coherent to both of the redundant channels may be inadvertently included if the coherence criterion is too low. When signal is much larger than noise at all frequencies, the in-phase power is identical to the single spectrum of either channel at all frequencies, proving that the phase shifts of the filters on the redundant channels differ by an insignificant amount.

Estimates of the dissipation rate were made by fitting the nondimensionalized response-corrected in-phase power to the one-dimensional Batchelor spectrum using a nonlinear least square fit. Each band-averaged spectral estimate was weighted by the number of frequencies in the band, insuring that the highest frequencies dominated the fit. This weighting is necessary because the low-frequency portion of the spectrum has few degrees of freedom and, as discussed by *Dillon and Caldwell* [1980*a*], the low-frequency region of the spectrum does not always increase linearly with frequency if the Cox number is of order 100 or less. We hypothesize that even without a distinct +1 frequency range, the dissipation rate can be obtained from the region of the peak, as long as a very distinct rolloff region is found.

In order for the fit to provide stable estimates, the spectrum must show a distinct peak and roll off sharply at the highest frequencies. If the spectrum has fallen to 10% of the peak value at f', we term the spectrum 'well-resolved,' since the fitting error is small. If the variance peak extends to higher frequencies and the spectrum has only fallen to between one third and one tenth of its peak value at f', we call the spectrum 'marginally resolved.' When the spectrum falls by less than a factor of 3, it is 'unresolved' and no estimate of the dissipation rate is made.

The fitting procedure can be thought of as adjusting the nondimensional frequency $\alpha = (2\pi f/U)k_B^{-1}(2q)^{1/2}$ and then changing the Batchelor wavenumber $k_B = (\varepsilon\nu^{-1}D^{-2})^{1/4}$ and hence the dissipation rate until the sum of the squared

differences between the measured spectrum and the Batchelor spectrum is a minimum. An upper bound on the error of the fit can be found by estimating the uncertainty of the spectrum at the highest frequency. If the slope of the Batchelor spectrum at f' is $dF(f')/df$, and the fractional uncertainty in spectral level at f' is $\delta S/S$, then the fractional uncertainty $\delta\alpha/\alpha$ will be approximately

$$\delta\alpha/\alpha = (\delta S/S)(dF(f')/df)$$

We assume that $\delta S/S$ is less than 20%, the maximum deviation from flatness of the response correction; $\delta\alpha/\alpha$ is then less than 0.04 for a well-resolved spectrum and less than 0.07 for a marginally resolved spectrum. Since the dissipation rate varies with the fourth power of α, the uncertainty in the dissipation rate estimate due to fitting error and spectral level uncertainties, $\delta\varepsilon/\varepsilon$, is smaller than 0.14 for the well-resolved spectrum and less than 0.28 for a marginally resolved spectrum.

A random uncertainty in drop speed $\delta U/U$ will introduce a random error of approximately $4\delta U/U$ in energy dissipation, because the drop speed is used to convert frequency to wavenumber by Taylor's hypothesis. We believe most drop speed fluctuations are due to large-scale internal waves [*Dillon and Caldwell*, 1980*b*] and that the sensor moves at a nearly constant rate relative to the immediately surrounding water. The drop speed was determined by averaging the speed for each cast within a series. The drop speeds were 10.7 cm/s, 12.1 cm/s, and 8.6 cm/s for series A, B, and C, respectively. (Although the same instrument was used for series A and B, the drop speeds differ because the angle of attack of the drag element was changed.) The variation in cast average drop speed among casts of the same series was 0.4 cm/s, and we take this to be the uncertainty in drop speed. This source of error introduces a random fractional uncertainty in dissipation rate of 0.13, 0.15, and 0.19 for series A, B, and C, respectively. Because the random variation in dissipation rate is much larger than this, we conclude that drop speed variations are not a significant source of error.

Turbulent velocity fluctuations can cause a broadening of the temperature gradient spectrum by causing random fluctuations in the Taylor speed. *Lumley* [1965] gives a method for finding a first-order estimate of the broadening. If the turbulent intensity (the ratio of the turbulent velocity variance to the square of the Taylor speed) is less than 0.01, corresponding in our case to a 1 cm/s rms turbulent velocity, the fractional error in dissipation introduced by broadening would be less than 0.11. If the turbulent intensity were as high as 0.05, corresponding to an rms turbulent velocity of approximately 2 cm/s, the fractional error would be less than 0.55. We have no objective measure of the turbulent intensity but believe this error to be small in most cases.

A systematic error in dissipation rate is possible because the value of the nondimensional number q [*Dillon and Caldwell*, 1980*a*] is not precisely known. We have used q = 3.5 for this study; *Oakey* [1982] found q = 3.7. Since the value of the dissipation rate varies with the square of q, our values would be underestimated by as much as 30% if q were as large as 4 or overestimated by as much as 35% if q were as small as 3. It is possible but unlikely that q is smaller than 3 or larger than 4.

The values for the molecular coefficients were not corrected for temperature changes. We used D = 0.0014 cm^2/s and ν = 0.01 cm^2/s throughout this report. While ν does change significantly with temperature and such variation can affect the kinetic energy dissipation rate calculation, such variations are almost always negligible when compared to the other sources of systematic error and to the sampling uncertainty in mean values. If, however, the listed values of dissipation rates in the tables are used for calculations other than those in this report, care should be taken to correct for the temperature dependence of viscosity.

Since the temperature variance dissipation rate is calculated from the integral of the spectrum and does not depend on Taylor's hypothesis or the fit to the Batchelor spectrum, the major source of error arises from the frequency response correction. Because errors in the 0–7-Hz band of the correction uniformly raise or lower the amplitude of the 7–30-Hz band without affecting the flatness in that band and because almost all of the variance lies in the 7–30-Hz band, the temperature variance dissipation rate estimate is sensitive to low-frequency error in the response correction, while the kinetic energy dissipation rate is not. As stated above, the low-frequency response may be overestimated. This low-frequency error would appear systematically in all the values of χ_T and in the buoyancy flux. An upper bound on this error is 30% and would be hardly noticeable in our figures.

An additional uncertainty in the temperature variance dissipation rate lies in the assumption of local isotropy. If the temperature gradients in the wavenumber range near the microstructure peak are entirely vertical, χ_T is overestimated by a factor of 3. Deviations from isotropy are expected to be small when the length scale at which the fluctuations are produced is much larger than the length scale of the smallest velocity fluctuations, but we do not know in a quantitative sense when anisotropies will be important.

Acknowledgments. The author would like to thank D. Caldwell for aiding and abetting this effort far beyond the call of duty. Sincere thanks are also given to J. Richman, R. deSzoeke, and C. Paulson, who were the source of many constructive discussions. The collection of microstructure data is a labor intensive project, and many deserve a vote of appreciation for their work: the inspiration and tireless effort of D. Caldwell was indispensible for the success of the MILE experiment, P. Newberger and M. Matsler aided in the collection of the oceanic data and S. Wilcox constructed the electronic equipment, and D. Caldwell, M. Brown, J. Richman, and M. Park spent many long hours helping with the collection of the freshwater data. The freshwater data collection and analysis were supported by the National Science Foundation under contract OCE-8018444. The MILE experiment and the analysis of the oceanic data were supported by the Office of Naval Research, contract N00014-79-C-0004.

REFERENCES

Batchelor, G. K., Small-scale variation of convected quantities like temperature in a turbulent fluid, *J. Fluid Mech.*, *5*, 113–133, 1959.

Businger, J. A., J. C. Wyngaard, Y. Izumi, and E. F. Bradely, Flux-profile relationships in the atmospheric surface layer, *J. Atmos. Sci.*, *25*, 1021–1025, 1971.

Caldwell, D. R., and T. M. Dillon, An oceanic microstructure measuring system, *Ref. 81-10*, School of Oceanogr., Oregon State Univ., 1981.

Caldwell, D. R., F. E. Snodgrass, and M. H. Wimbush, Sensors in the deep sea, *Phys. Today*, *22*, 34–42, 1969.

Caldwell, D. R., S. D. Wilcox, and M. Matsler, A relatively simple freely-falling probe for small-scale temperature gradients, *Limnol. Oceanogr.*, *20*, 1035–1047, 1975.

Dillon, T. M., and D. R. Caldwell, The Batchelor spectrum and dissipation in the upper ocean, *J. Geophys. Res.*, *85*, 1910–1916, 1980*a*.

Dillon, T. M., and D. R. Caldwell, High-frequency internal waves at Ocean Station P, *J. Geophys. Res.*, *85*, 3277–3284, 1980*b*.
Gibson, C. H., Alternative interpretations for microstructure patches in the thermocline, *J. Phys. Oceanogr.*, *12*, 374–383, 1982.
Gregg, M. C., and T. Meagher, The dynamic response of glass rod thermistors, *J. Geophys. Res.*, *85*, 2779–2786, 1980.
Lumley, J. L., Interpretation of time spectra measured in high-intensity shear flows, *Phys. Fluids*, *8*, 1056–1062, 1965.
Oakey, N. S., Determination of the rate of dissipation of turbulent energy from simultaneous temperature and velocity shear microstructure measurements, *J. Phys. Oceanogr.*, *12*, 256–271, 1982.
Osborn, T. R., Estimates of the local rate of vertical diffusion from dissipation measurements, *J. Phys. Oceanogr.*, *10*, 83–89, 1980.
Osborn, T. R., and C. S. Cox, Oceanic finestructure, *Geophys. Fluid Dyn.*, *3*, 321–345, 1972.
Simons, T. J., Development of three-dimensional numerical models of the Great Lakes, *Sci. Ser. 12*, Inland Waters Directorate, Canada Centre for Inland Waters, Burlington, Ont., Canada, 1973.
Stillinger, D. C., An experimental study of the transition of grid turbulence to internal waves in a salt-stratified water channel, Ph.D. dissertation, Univ. of Calif., San Diego, 1981.
Tennekes, H., and J. L. Lumley, *A First Course in Turbulence*, Massachusetts Institute of Technology Press, New York, 1972.
Thorpe, S. A., Turbulence and mixing in a Scottish Loch, *Philos. Trans. R. Soc. London Ser. A*, *286*, 125–181, 1977.

(Received January 4, 1982;
revised July 19, 1982;
accepted August 27, 1982.)